https://doi.org/10.5194/egusphere-2026-3750
Preprint. Discussion started: 7 July 2026

Comparative Nitrogen Speciation in Marine and Coastal Urban Aerosols of the Greater Bay Area and Ecosystem Implications

Cong Cao[1], Wei Chen[2], Xu Yu[2,3], Wing Hei Marco Wong[1], Ningning Sun[4], Kun Zhang[2], Weicong Cheng[5], Jianping Gan[5,6], Jian Zhen Yu[1,2*]

1. Department of Chemistry, Hong Kong University of Science & Technology, Clear Water Bay, Kowloon, Hong Kong, 999077, China
2. Division of Environment and Sustainability, Hong Kong University of Science & Technology, Clear Water Bay, Kowloon, Hong Kong, 999077, China
3. Now at Jiangsu Collaborative Innovation Center of Atmospheric Environment and Equipment Technology, Jiangsu Key Laboratory of Atmospheric Environment Monitoring and Pollution Control, School of Environmental Science and Engineering, Nanjing University of Information Science and Technology, Nanjing, 210044, China
4. Key Lab of Geographic Information Science of the Ministry of Education, School of Geographic Sciences, East China Normal University, Shanghai, 210062, China
5. Department of Ocean Science, Hong Kong University of Science & Technology, Clear Water Bay, Kowloon, Hong Kong, 999077, China
6. Center for Ocean Research in Hong Kong and Macau, Hong Kong University of Science & Technology, Clear Water Bay, Kowloon, Hong Kong, 999077, China

Correspondence to: Jian Zhen Yu (jian.yu@ust.hk)

Abstract. We present a summer 2024 comparative study of aerosol nitrogen speciation across the Guangdong–Hong Kong–Macau Greater Bay Area (GBA), contrasting marine air over the coastal ocean with a coastal urban site in Hong Kong. Inorganic nitrogen (IN) and organic nitrogen (ON) were quantified, and a high-resolution time-of-flight aerosol mass spectrometer was operated offline to characterize water-soluble nitrogen-containing organics. Total nitrogen and IN showed a west-to-east increase along the coastal ocean, indicating stronger anthropogenic influence in the more populated eastern GBA. ON showed a contrasting pattern: while its concentration decreased offshore, its fraction in total nitrogen peaked in the western marine region (34.6 ± 12.4%), highlighting the relative importance of ON under lower $PM_{2.5}$ loadings. Urban aerosols were enriched in ammonium and exhibited more oxidized ON signatures, including higher NO^+/NO_2^+ ratios (7.9 ± 2.6), consistent with NO_x–VOC photochemistry. Marine aerosols showed lower NO^+/NO_2^+ ratios (5.3 ± 1.3) and molecular signatures consistent with reduced, amine-related ON, reflecting marine biogenic inputs in the marine boundary layer. Using an inferential approach with deposition velocity (V_d) assumptions, $PM_{2.5}$-bound nitrogen deposition over the ocean was estimated to be comparable to that at the urban site (0.14 vs. 0.15 kg N ha^{-1} yr^{-1}), indicating non-negligible fine-particle nitrogen input to adjacent coastal waters. These results demonstrate a notable coastal transition in nitrogen chemical form and suggest that ON speciation should be considered when assessing nitrogen deposition to coastal waters and potential ecosystem responses in the South China Sea.

Keywords. Offline aerosol mass spectrometry, reduced/oxidized organic nitrogen, shipping emissions, coastal urban atmosphere, nitrogen deposition, marine ecosystem impact

https://doi.org/10.5194/egusphere-2026-3750
Preprint. Discussion started: 7 July 2026

1. Introduction

Atmospheric aerosol nitrogen plays a critical role in marine nutrient cycles and coastal air quality, particularly over the coastal and offshore areas strongly influenced by both continental outflows and local emissions (Jickells et al., 2013; Mahowald et al., 2017; Luo et al., 2018). Reactive nitrogen species emitted from combustion, agriculture, and natural sources, such as soils, lightning, and the ocean, can undergo atmospheric transformations and eventually deposit on terrestrial and aquatic ecosystems (Palta and Hartnett, 2018; Galloway et al., 2008). Their deposition rates depend strongly on chemical speciation and physical phase. In coastal and ocean regions, atmospheric deposition of reactive nitrogen can stimulate phytoplankton productivity, but excessive nitrogen inputs may also promote eutrophication, harmful algal blooms (HAB), and the expansion of hypoxic dead zones (Howarth and Marino, 2006; Anderson et al., 2002; Diaz and Rosenberg, 2008; Lee et al., 2019; Yau et al., 2020). Meanwhile, ocean–atmosphere exchange processes (such as oceanic ammonia and amine emissions) feed back into the atmospheric nitrogen cycle, creating a tightly coupled land–atmosphere–ocean nitrogen budget (Paulot et al., 2015; Zhang et al., 2023).

Traditionally, nitrate (NO_3^-) was the dominant form of inorganic nitrogen (IN) in ambient particulate matter (PM), primarily linked to fossil fuel combustion and industrial NO_x emissions. However, recent findings reveal a shifting chemical profile in southern China, where ammonium (NH_4^+), derived mainly from agricultural NH_x (NH_3 + NH_4^+), now exceeds NO_3^- as the major contributor to aerosol N. This transition is attributed to two concurrent trends: rising NH_3 emissions due to intensified agricultural activities (e.g., fertilizer use, livestock waste), and declining NO_x emissions following improved air pollution controls on coal combustion and industry (Zhang et al., 2024b).

Organic nitrogen (ON) is emerging as a significant and understudied contributor to the total reactive nitrogen budget, contributing approximately 25–30% of total nitrogen deposition on a global scale (Jickells et al., 2013; Duce et al., 2008). Atmospheric ON includes a wide range of compounds such as urea, amines, amino acids, amides, N-heterocyclics, nitroaromatic compounds, nitro-polycyclic aromatic hydrocarbons (nitro-PAHs), and organic nitrates (Yu et al., 2024). These can be either directly emitted from biomass burning, fossil fuel combustion, marine biological activity, and soil sources or formed through atmospheric reactions of volatile organic compounds (VOCs) in the presence of NO_x or NH_3/NH_4^+. In marine and coastal atmospheres, aerosol ON has multiple sources, including marine biological emissions, transported terrestrial and anthropogenic inputs, and secondary atmospheric processing. As an important component of atmospheric nitrogen, aerosol ON can vary notably in both concentration and relative contribution to total aerosol nitrogen, depending on region, air-mass origin, and particle size (Jickells et al., 2013). Based on observations at Bermuda in the Atlantic Ocean, Altieri et al. (2016) further showed that the ON in marine aerosols was strongly associated with surface-ocean biological activity and wind-driven aerosol generation, highlighting a marine biogenic source under remote marine conditions.

https://doi.org/10.5194/egusphere-2026-3750
Preprint. Discussion started: 7 July 2026

The Guangdong–Hong Kong–Macau Greater Bay Area (GBA) is one of the most densely populated and economically vibrant urban clusters in China, comprising 11 core cities, including Guangzhou, Shenzhen, Hong Kong, and Macau. Although it occupies less than 1% of the national land area, the GBA contributes over 10% of China's GDP, supported by intensive manufacturing, high-tech industries, and a rapidly expanding service sector (Zhang et al., 2020; Hui et al., 2020; Park and Song, 2021). The combination of high urbanization, vehicle traffic, industrial emissions, and energy consumption makes the GBA a significant hotspot for reactive nitrogen emissions, including NO_x, NH_3, and various ON compounds. Its location along the South China Sea, together with frequent exposure to monsoonal flows, also makes the region a natural laboratory for studying interactions between marine emissions and urban nitrogen pollution and for understanding how nitrogen speciation varies among air masses with different source influences. Despite the regional significance of the GBA, observations of aerosol nitrogen species, especially over the oceanic domain, remain very limited. There is a need to quantify both IN and ON in marine and coastal air masses, characterize their transformations, and assess their relative contributions to TN deposition in this dynamic environment.

To address these data gaps, we characterized marine nitrogenous aerosol composition using samples collected during a summer 2024 cruise campaign over GBA coastal waters and compared the observations with those from a coastal urban site in Hong Kong. Filter-based measurements were used to quantify IN and ON, water-soluble ions, and water-soluble bulk nitrogen, complemented by offline aerosol mass spectrometry (AMS) characterization of the water-extracted fraction. The objectives were to (1) characterize differences in aerosol bulk N fractions (ON vs. IN) between marine and coastal urban air, (2) determine the relative importance of oxidized vs. reduced ON in these contrasting environments using AMS measurements, and (3) evaluate implications for nitrogen deposition and marine nutrient inputs. Our observations provide new constraints on the spatial variability, chemical characteristics, and potential sources of aerosol nitrogen in the GBA, with relevance for understanding nitrogen deposition in coastal mega-regions and improving regional nitrogen budgets and chemical transport modeling.

2. Cruise campaign and chemical analysis methods

2.1 Cruise campaign description

The cruise campaign was carried out from 12 July to 3 August 2024 over the GBA coastal water (Nuruddin et al., 2026), as part of a broader interdisciplinary survey (Earth-HK, https://earthhk.hkust.edu.hk/), which was designed to investigate the regional earth system of the GBA with an emphasis on coupled land–ocean–atmosphere processes. The overall campaign collected a multidisciplinary dataset, including physical and biogeochemical oceanographic measurements and atmospheric observations. Here, we focus on atmospheric aerosol samples collected during the cruise to characterize the nitrogen speciation and chemical composition of aerosols over adjacent marine

https://doi.org/10.5194/egusphere-2026-3750
Preprint. Discussion started: 7 July 2026

regions. The research cruise (Lan Bo 3) departed from Hong Kong waters and sailed across three oceanic regions A, B, and C (Fig. 1). These regions were chosen to capture gradients in air mass characteristics, including relatively clean maritime background conditions, areas influenced by continental outflow, and zones affected by regional shipping activity. The cruise track included several intersecting and partially overlapping transects within and between the three regions, reflecting practical navigation routes, transitions among sampling areas, and adjustments made in response to weather conditions and operational requirements.

The campaign period coincided with the prevailing southwesterly monsoonal flow, typically bringing in clean maritime air, interspersed with occasional continental outflow episodes. This seasonal setting provided an opportunity to characterize the chemical composition and nitrogen speciation of marine aerosols under anthropogenic influence from the surrounding coastal megacity cluster.

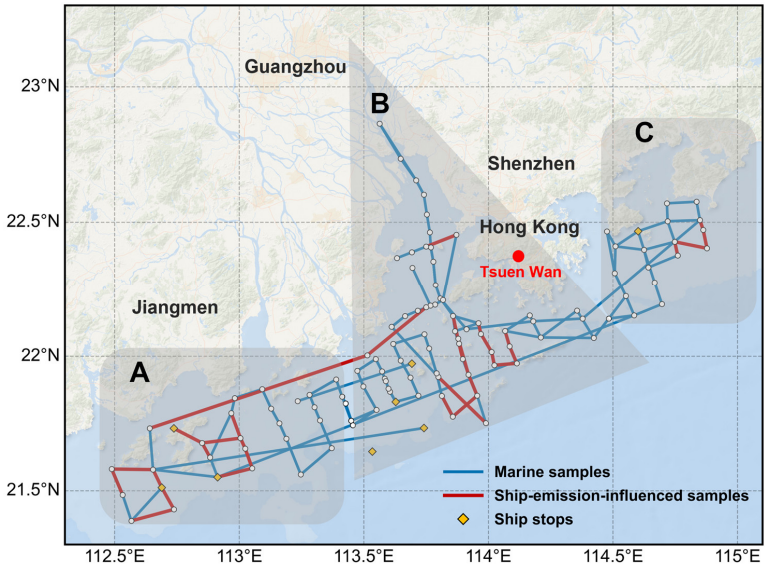

Figure 1. Spatial distribution of cruise sampling routes in the GBA water. Blue routes indicate marine samples retained for analysis, whereas red routes indicate samples identified as ship-emission-influenced. The red dot marks the Tsuen Wan coastal urban site in Hong Kong. White dots denote short ship stops (mainly for oceanographic experiments) when the high-volume air sampler was suspended, whereas yellow diamonds denote longer stationary or anchoring periods, including typhoon-related sheltering and other operational stops, during which sampling was maintained. The shaded areas labeled A–C define the three marine sampling regions used for regional comparison. Basemap source: Esri World Ocean Base; © Esri, Garmin, GEBCO, NOAA NGDC, and other contributors | Powered by Esri.

2.2 Aerosol sample collection

A total of 91 ambient $PM_{2.5}$ aerosol samples were collected over the GBA coastal waters during the cruise campaign, using a high-volume air sampler (1.13 m^3 min^{-1}; Thermo Fisher Scientific, USA). Aerosols were collected on prebaked quartz fiber filters (550 °C, 8 h). The sampler was mounted on the upper deck of the research vessel, with its location shown in Fig. S1, and was positioned away from exhaust outlets to minimize the direct influence of ship emissions. Sampling was conducted only when the vessel was underway and was suspended when the ship was docked or idle. However, sampling was

https://doi.org/10.5194/egusphere-2026-3750
Preprint. Discussion started: 7 July 2026

maintained during unavoidable anchoring or stationary periods, such as typhoon-related sheltering and other operational stops (Fig. 1), and all samples were subsequently screened for potential ship-emission influence based on NO_x measurements discussed below. The sampling duration of individual filters ranged from 1.2 to 17.1 h, with an average of 3.8 ± 2.8 h (Table S3), to ensure sufficient $PM_{2.5}$ mass for subsequent chemical analysis. Immediately after collection, filters were wrapped in aluminum foil, sealed in airtight containers, and stored at –18 °C until analysis.

Despite these precautions, some samples may still have been influenced by ship emissions under certain wind conditions. To identify such contamination, we operated a chemiluminescence NO_x analyzer (model 42i-TL, Thermo Scientific, USA) with one-minute resolution throughout the campaign. The NO_x analyzer was located on the second deck, while the high-volume sampler was installed on the third (uppermost) deck outside the bridge; their inlets were separated by approximately 2 m vertically and 10 m horizontally (Fig. S1). Given this close proximity, the NO_x record served as a practical indicator of ship-exhaust influence on the concurrent $PM_{2.5}$ samples. A filter sample was classified as contaminated if NO_x concentrations exceeded 100 ppb for at least a 10-minute period during its sampling. By this criterion, 16 of the 91 samples were excluded. These excluded samples also exhibited significantly higher total carbon (TC) concentrations than the uncontaminated marine samples (Fig. S2). All subsequent analyses were based on the remaining 75 samples.

In parallel, 23 daily $PM_{2.5}$ samples were collected at the Tsuen Wan air quality monitoring station (22°22′18 N, 114°6′52 E) in Hong Kong between 12 July and 3 August 2024. This site represents a densely populated coastal urban environment affected by both local traffic emissions and regional transport (Chow et al., 2022). Sampling was conducted using the same type of high-volume air sampler as that used during the cruise, and an identical filter preparation protocol was followed, ensuring methodological consistency between marine and urban measurements. The Tsuen Wan dataset enables direct comparison of aerosol composition between marine and urban environments in the GBA. For comparison of nitrate and ammonium, hourly online ion chromatography (IC) system measurements at the Tsuen Wan site were used to represent urban aerosol-phase NO_3^- and NH_4^+, as described in Section 2.3.2.

2.3 Chemical analysis

The collected $PM_{2.5}$ samples were subjected to a suite of chemical analyses to determine their nitrogenous and carbonaceous components.

2.3.1 IN and ON determined by the aerosol nitrogen analyzer system

The concentrations of aerosol IN and ON were quantified using the thermal evolution–chemiluminescence method, following the protocol described by Yu et al. (2021). Briefly, filter punches were heated in an oxygen flow at stepwise temperatures to release nitrogen-containing species in different volatility fractions. The evolved gases were separated into two streams: one passed through a methanator, where CO_2 was catalytically converted to CH_4 and the carbon signal quantified by a flame

https://doi.org/10.5194/egusphere-2026-3750
Preprint. Discussion started: 7 July 2026

ionization detector; the other passed through a molybdenum catalytic converter, where various nitrogen oxides (NO_y) were reduced to NO and subsequently detected by chemiluminescence using a NO_x analyzer. IN (primarily nitrate and ammonium) was released at lower temperatures, while ON species were released at higher temperatures. The combined carbon–nitrogen detection enables identification of IN and ON, as ON aerosols exhibit concurrent carbon and nitrogen signals, whereas IN yields only nitrogen. Their distinct thermal-release profiles further aid discrimination. Quantification of each fraction is then accomplished by applying multivariate curve resolution (MCR) to the temperature-resolved C and N signals, providing a robust separation beyond that achievable by thermal evolution alone. The method and instrument details are documented in Yu et al. (2021).

2.3.2 Water-soluble ions determined by the IC

For the determination of major water-soluble inorganic ions (e.g., Na^+, NH_4^+, K^+, Mg^{2+}, Ca^{2+}, Cl^-, NO_3^-, SO_4^{2-}) in the marine $PM_{2.5}$ filter samples, a separate portion of each quartz filter was extracted in ultrapure water under ultrasonication. The extracts were filtered and analyzed using ion chromatography (IC) (Dionex, Thermo Scientific, USA). Calibration was carried out using multi-ion standards, and field blanks were processed in parallel to correct background contamination.

For the Tsuen Wan urban site, aerosol-phase NO_3^- and NH_4^+ were obtained from a Monitor for AeRosols and Gases in ambient Air (MARGA, Metrohm Applikon), an online IC system operated at hourly time resolution (Zhang and Yu, 2026). Compared with the daily $PM_{2.5}$ filter samples, the online MARGA measurements provide higher temporal resolution and avoid analytical artifacts that are known for ammonium nitrate due to its semi-volatile nature-induced loss during filter sampling and storage. Therefore, MARGA-derived NO_3^- and NH_4^+ were used for the analysis of urban inorganic ions. Nitrate and ammonium were converted to nitrogen-equivalent concentrations, expressed as $N\text{–}NO_3^-$ and $N\text{–}NH_4^+$, using their respective nitrogen mass fractions.

2.3.3 Water-soluble carbon and nitrogen determined by the total organic carbon and total nitrogen (TOC/TN) analyzer

Another aliquot of the water extracts was analyzed for water-soluble organic carbon (WSOC) and water-soluble total nitrogen (WSTN) using a Shimadzu TOC/TN analyzer (Shimadzu, Japan). The instrument quantifies the total WSOC by catalytic combustion and non-dispersive infrared detection of CO_2, while WSTN is measured by chemiluminescence detection of NO formed after high-temperature combustion.

2.3.4 Offline AMS Measurements

The offline AMS method used in this study was adapted from Daellenbach et al. (2016) and Vlachou et al. (2018), with some modifications to the sample preparation and aerosolization process. In brief, water-soluble components of $PM_{2.5}$ samples (23 urban samples, 47 marine samples, and 4 ship-emission-influenced samples) were analyzed using a high-resolution time-of-flight aerosol mass spectrometer (HR-ToF-AMS). Each quartz filter sample was extracted with 15 mL of ultrapure water

https://doi.org/10.5194/egusphere-2026-3750
Preprint. Discussion started: 7 July 2026

via ultrasonic agitation. The water extracts were subsequently aerosolized using a custom-built atomizer optimized for small-volume nebulization. During atomization, a stream of ultra-high purity (UHP) argon gas served as the carrier, directly passing through the atomizer to generate aerosols without additional air filtration. The argon flow entrained the water solution, forming submicron droplets that were dried using a silica gel diffusion dryer to remove residual water content. The resulting dry particles were then introduced into the HR-ToF-AMS (operated in W-mode) for analysis. For each sample, mass spectra were recorded over the 12–300 amu range, with a collection time of 60 seconds per spectrum. Between each sample run, ultrapure water was nebulized to assess system background and minimize potential memory effects. Field blanks were processed using the same protocol and showed signals comparable to those obtained from ultrapure water alone, confirming negligible contamination.

The HR-ToF-AMS provides quantitative mass spectra of non-refractory $PM_{2.5}$ components (e.g., organics, ammonium, sulfate, nitrate), with the vaporizer operated at 600 °C under a vacuum of ~10^{-7} Torr. Data analysis was conducted using high-resolution fitting tools SQUIRREL (v1.62G) and PIKA (v1.22G) within the IGOR Pro software package (WaveMetrics Inc., Portland, OR, USA), following standard protocols as described by Decarlo et al. (2006).

Reduced organic nitrogen (amines, amides, amino acids, and imidazole-like heterocycles) in the water extraction was identified using characteristic fragment ions, based on standard spectra (Ge et al., 2024). Amines were diagnosed by $C_nH_{2n+2}N^+$ ions (e.g., CH_4N^+, $C_2H_6N^+$, $C_3H_8N^+$, and $C_4H_{10}N^+$), while amides were characterized by $C_nH_{2n}NO^+$ fragments (e.g., CH_2NO^+, $C_3H_6NO^+$, and $C_4H_8NO^+$), reflecting the –CONH– functional group. Amino acids were identified based on the concurrent presence of CH_4NO^+, $C_2H_3NO^+$, and $C_2H_4NO_2^+$ ions. Imidazole-like heterocycles were determined by $C_xH_yN_2^+$ ions (e.g., $C_3H_3N_2^+$ and $C_3H_4N_2^+$), characteristic of N-heterocyclic ring structures (Zhang et al., 2024a). Although individual fragments (e.g., CH_4N^+ and CH_2NO^+) may originate from multiple N-containing species, the combined use of these diagnostic ions provides a robust semi-quantitative functional-group-level classification of water-soluble reduced nitrogen.

In addition to reduced organic nitrogen, oxidized organic nitrogen functionalities were assessed using the NO^+/NO_2^+ ratio derived from the HR-ToF-AMS spectra. This ratio has been widely applied to distinguish organic nitrates and nitro-compounds from inorganic nitrate, as oxidized ON species typically exhibit elevated NO^+/NO_2^+ values (~8.6–15) (Ge et al., 2024; Farmer et al., 2010; Graeffe et al., 2023), whereas inorganic nitrate (e.g., NH_4NO_3) shows substantially lower ratios (~2.4–2.7) (Bruns et al., 2010; Fry et al., 2009). The NO^+/NO_2^+ ratio thus serves as a diagnostic indicator for the relative contribution of oxidized ON in the water-soluble aerosol fraction.

2.4 Aerosol N deposition calculation

The dry N deposition flux from $PM_{2.5}$ is estimated by using the inferential method by Eq. (1):

$$F = C_a \times V_d , \quad (1)$$

https://doi.org/10.5194/egusphere-2026-3750
Preprint. Discussion started: 7 July 2026

where F (mg N m^{-2} s^{-1}) is the dry deposition flux of an N species (e.g., nitrate, ammonium), C_a (mg N m^{-3}) is the ambient concentration, and V_d (m s^{-1}) is the dry deposition velocity of the species. C_a was from direct measurement, while V_d was estimated based on the particle dry-deposition calculation method of Zhang et al. (2001), using representative particle and surface parameters for the marine and coastal urban environments, as described in Section 3.4 and the Supplement.

3. Results and discussion

3.1 Spatial distribution of aerosol nitrogen and related species over the GBA water

The regional pattern and offshore evolution of aerosol nitrogen over the GBA coastal waters are summarized in Fig. 2. Panel (a) presents the spatial distributions of IN and ON concentrations along the cruise track. Panels (b) and (c) show the offshore gradients of IN and ON, respectively, as a function of distance from the nearest coastline, after the samples were grouped by offshore distance. Solid lines represent Sen's slopes, and the Mann–Kendall test statistics are used to evaluate the significance of the monotonic trends. $PM_{2.5}$ samples were grouped into three representative regions based on cruise track locations: (A) western coastal waters (west of the Pearl River Estuary), (B) the Pearl River Estuary region, and (C) eastern coastal waters, including Mirs Bay and Daya Bay (Fig. 2a).

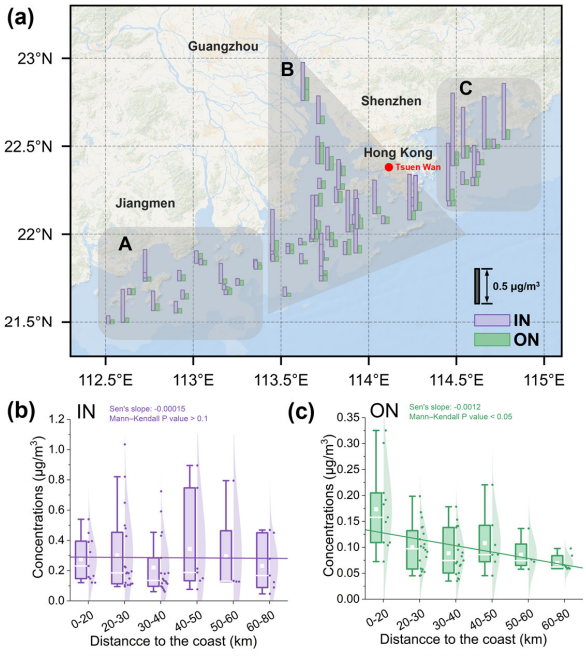

Figure 2. (a) Spatial distributions of IN (purple bar) and ON (green bar) concentrations in $PM_{2.5}$ samples collected during the research cruise campaign over the GBA oceanic region during summer 2024. Basemap source: Esri World Ocean Base; © Esri, Garmin, GEBCO, NOAA NGDC, and other contributors | Powered by Esri. (b-c) Offshore gradients of IN and ON in $PM_{2.5}$, as a function of distance to the coastline (the line in each figure represents Sen's slope, and the Mann–Kendall tests are used to quantify the significance of the offshore trends).

https://doi.org/10.5194/egusphere-2026-3750
Preprint. Discussion started: 7 July 2026

A clear spatial gradient of west-to-east increase was observed in IN and TN concentrations (Fig. 2a; Table 1), with TN increasing from 0.25 ± 0.13 μg m^{-3} in region A to 0.41 ± 0.23 μg m^{-3} in region B and to 0.56 ± 0.40 μg m^{-3} in region C. IN (composed predominantly of NO_3^-, and NH_4^+) followed the same spatial trend, consistent with intensified anthropogenic emissions and secondary aerosol formation toward the urbanized eastern GBA, where dense shipping, traffic, and industrial activity elevate NO_x and NH_3. The accompanying inorganic and carbonaceous components reinforce this picture: NO_3^-, NH_4^+, EC, OC, and WSOC all peaked in region C, indicating enhanced secondary inorganic and organic aerosol loading. SO_4^{2-}, in contrast, showed a weaker, non-monotonic pattern with comparable levels in regions A and B and slightly lower values in region C, suggesting that sulfate during this campaign was shaped more by regional background transport and marine boundary-layer processing than by the west–east anthropogenic gradient.

Table 1. Concentrations (average ± standard deviation) of IN and ON as well as ON/TN ratio, major inorganic ions, carbonaceous components (OC, EC, WSOC), and WSTN in $PM_{2.5}$ samples from three marine regions (A, B, C) over the GBA.

Region	A	B	C
I. IN (μg m^{-3}), ON (μg m^{-3}), TN (μg m^{-3}), ON/TN (%)			
IN	0.17 ± 0.13	0.30 ± 0.20	0.45 ± 0.35
ON	0.07 ± 0.02	0.12 ± 0.06	0.11 ± 0.05
TN	0.25 ± 0.13	0.41 ± 0.23	0.56 ± 0.40
ON/TN	34.6 ± 12.4	31.9 ± 13.4	26.9 ± 13.1
II. Inorganic Ions (μg m^{-3})			
Cl^-	0.19 ± 0.10	0.22 ± 0.19	0.24 ± 0.25
SO_4^{2-}	2.21 ± 0.97	2.31 ± 0.93	1.95 ± 0.45
NO_3^-	0.38 ± 0.29	0.57 ± 0.41	0.58 ± 0.47
Na^+	0.34 ± 0.40	0.33 ± 0.20	0.24 ± 0.12
NH_4^+	0.19 ± 0.19	0.22 ± 0.24	0.25 ± 0.15
K^+	0.14 ± 0.04	0.17 ± 0.08	0.11 ± 0.01
Mg^{2+}	0.08 ± 0.03	0.11 ± 0.05	0.07 ± 0.01
Ca^{2+}	0.09 ± 0.05	0.17 ± 0.27	0.08 ± 0.03
III. OC, EC, WSOC, WSTN (μg m^{-3})			
OC	2.42 ± 1.34	3.27 ± 1.79	3.38 ± 1.81
EC	0.46 ± 0.53	0.60 ± 0.50	0.55 ± 0.41
WSOC	1.42 ± 0.69	2.58 ± 3.41	2.74 ± 2.10
WSTN	0.30 ± 0.13	0.43 ± 0.23	0.59 ± 0.38

ON exhibited the opposite pattern in relative importance. Although absolute ON concentrations were low across all regions, the ON/TN ratio was highest in the more marine-influenced region A (34.6 ± 12.4%) and decreased eastward (B: 31.9 ± 13.4%; C: 26.9 ± 13.1%). This inverse relationship between ON/TN and TN indicates that the rising anthropogenic IN, rather than a sharp decline in ON itself, drives the eastward drop in the relative contribution of ON, while natural primary sources, such as oceanic biogenic emissions, organic-matter photodegradation, and sea-spray–associated organics, sustain a meaningful ON fraction under cleaner conditions. Comparable ON contributions (~30%) have

https://doi.org/10.5194/egusphere-2026-3750
Preprint. Discussion started: 7 July 2026

been reported for the South China Sea, with the majority of water-soluble ON residing in the fine fraction (Shi et al., 2010), reinforcing that ON remains an important component of coastal and marine fine-aerosol nitrogen even as anthropogenic N inputs decline.

To quantify offshore gradients in aerosol nitrogen, the 75 marine samples were grouped into six distance bins (0–20, 20–30, 30–40, 40–50, 50–60, and 60–80 km from the nearest coastline), capturing the transition from coastal outflow to marine background. Trends across bins were evaluated using Theil–Sen regression (Wilcox, 2017) for robust slope estimation, the Mann–Kendall test (Wang et al., 2020) for significance, and Kendall's τ for monotonicity strength.

Both IN and ON declined with offshore distance (Fig. 2b, 2c), reflecting dilution of terrestrial influence in the marine boundary layer, but the two species behaved very differently. ON showed a strong, coherent gradient (Sen's slope = -1.23×10^{-3} μg m^{-3} km^{-1}, or ~0.012 μg m^{-3} per 10 km; $\tau = -0.73$; $p < 0.05$), whereas IN showed essentially no monotonic trend (Sen's slope = -1.49×10^{-4} μg m^{-3} km^{-1}, nearly an order of magnitude smaller; $\tau = -0.07$; $p > 0.1$). This contrast indicates that marine ON is dominated by continental sources, including reduced nitrogen and nitrogen-containing VOCs that partition into particulate ON after oxidation (Ng et al., 2017; Farmer et al., 2010; Nie et al., 2022; Cape et al., 2011), and is rapidly attenuated during marine transport. IN, by comparison, is buffered by efficient secondary production and longer atmospheric lifetimes (Seinfeld and Pandis, 2016; Kanakidou et al., 2012), producing a more spatially homogeneous regional-background field. The sharp offshore decay of ON, therefore, underscores the dominant role of land-based anthropogenic emissions in setting marine ON loading and deposition over the GBA coastal ocean.

Overall, the eastward increase in aerosol TN across the GBA marine region reflects stronger anthropogenic emissions along the more urbanized eastern coast, whereas the opposing ON/TN pattern points to distinct source controls. Specifically, ON is dominated by terrestrial sources that attenuate rapidly offshore during marine transport, while IN reflects regional-scale secondary formation with a longer atmospheric lifetime. Assessing nitrogen inputs to coastal marine environments therefore requires considering both the magnitude and the chemical composition of aerosol nitrogen.

3.2 Contrasting characteristics of IN and ON in marine and urban aerosols

Atmospheric IN and ON over coastal oceans are shaped by the combined influence of continental outflow, regional photochemistry, and marine boundary layer processing (Altieri et al., 2016; Kanakidou et al., 2016). The $PM_{2.5}$ samples collected over the GBA coastal ocean and a nearby coastal urban site in Hong Kong provide a paired dataset for examining contrasts and commonalities in IN and ON under closely coupled marine–urban conditions. Figure 3 provides an overview of the campaign-scale temporal variability and distributional differences of $PM_{2.5}$-bound nitrogen species between the marine and urban environments, including bulk IN and ON concentrations and the partitioning of inorganic nitrogen between nitrate and ammonium.

https://doi.org/10.5194/egusphere-2026-3750
Preprint. Discussion started: 7 July 2026

At the bulk level, both IN and ON exhibited broadly comparable concentrations and temporal variability between marine and urban samples (Fig. 3a, 3b), indicating nitrogen-containing aerosols over the coastal ocean are not controlled by local marine emissions alone but are strongly influenced by regional transport and large-scale atmospheric processing extending across the GBA marine boundary layer. In both environments, ammonium nitrogen ($N–NH_4^+$) exceeded nitrate nitrogen ($N–NO_3^-$), but the relative balance differed markedly (Fig. 3c-f). Marine samples showed a moderate NH_4^+-dominant composition (campaign-mean $N–NH_4^+/N–NO_3^-$ ratio ≈ 1.8), whereas the urban MARGA data yielded a substantially larger ratio of ~5.4, indicating a much stronger NH_4^+-rich regime at the urban site. The appreciable $N–NO_3^-$ observed in marine $PM_{2.5}$ suggests that nitrate was not simply suppressed offshore. Instead, it likely reflects sea-salt processing via chloride displacement [$HNO_3(g) + NaCl(s) \rightarrow NaNO_3(s) + HCl(g)$] (Guimbaud et al., 2002; Davies and Cox, 1998), which shifts nitrate from the gas to the particle phase. Although much of the reacted nitrate resides in coarse particles, chloride-depleted fine sea salt and internally mixed marine particles can also contribute to the $PM_{2.5}$ fraction. This interpretation is supported by the Na^+ data: mean Na^+ was 0.36 ± 0.35 μg m^{-3} in marine $PM_{2.5}$ versus 0.16 ± 0.10 μg m^{-3} at the urban site (marine mean ≈ 2.3 × urban), confirming greater sea-salt influence over the ocean.

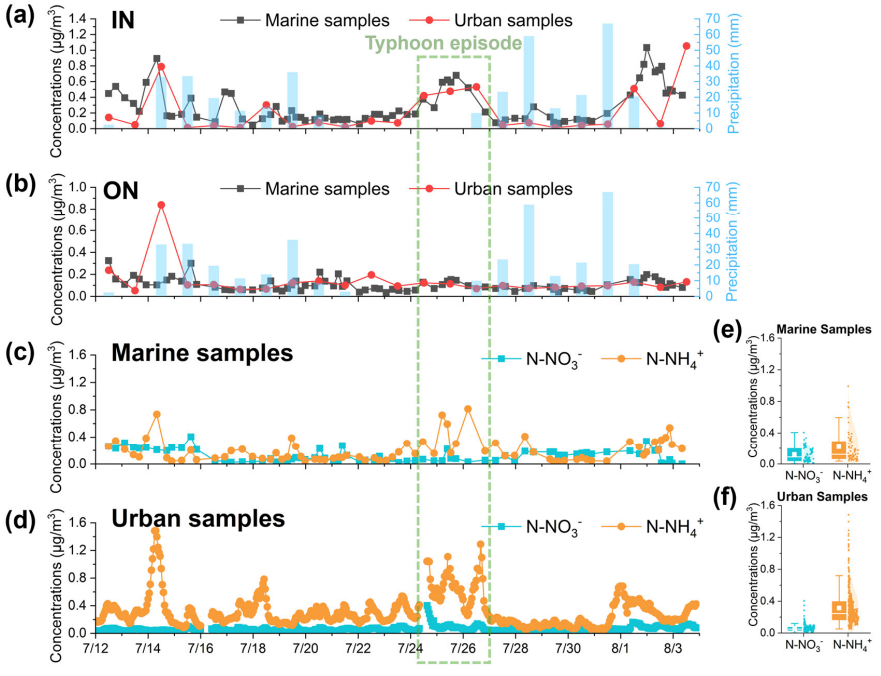

Figure 3. Temporal variations of (a) IN and (b) ON concentrations in marine (black squares) and urban (red circles) $PM_{2.5}$ filter samples during the 2024 summer campaign. Blue bars indicate daily precipitation in Hong Kong (right axis). Panels (c) and (e) show the time series and distributions of nitrate nitrogen ($N–NO_3^-$) and ammonium nitrogen ($N–NH_4^+$) in marine $PM_{2.5}$ samples based on filter-based IC measurements. Panels (d) and (f) show the corresponding time series and distributions of $N–NO_3^-$ and $N–NH_4^+$ at the Tsuen Wan urban site based on hourly MARGA measurements.

https://doi.org/10.5194/egusphere-2026-3750
Preprint. Discussion started: 7 July 2026

During the typhoon-influenced period (24–26 July 2024), pronounced meteorological perturbations were observed, including a sharp drop in sea-level pressure, sustained strong winds with rapidly shifting wind directions, and episodic precipitation (Fig. S3), indicative of the passage of the typhoon system and associated circulation changes. Against this background, IN concentrations, dominated by $N–NH_4^+$, were elevated relative to campaign-average levels, particularly in marine samples. Back-trajectory analysis (Fig. 4) showed alternating southwest and northwest transport pathways during this episode, indicating that continental/inland air masses carried elevated NH_3 from high-emission source regions, which subsequently enhanced particulate NH_x through gas-to-particle partitioning. Offline AMS fragment analysis corroborates this enhancement. NH_x accounted for a markedly larger fraction of N-containing fragments during 24–26 July than in other periods, particularly in marine samples (Fig. S4). In contrast, ON concentrations remained relatively stable during the typhoon episode, suggesting that bulk ON was less sensitive than IN to short-term meteorological variability and air-mass switching, and was instead governed primarily by regional background sources and longer-lived atmospheric processing.

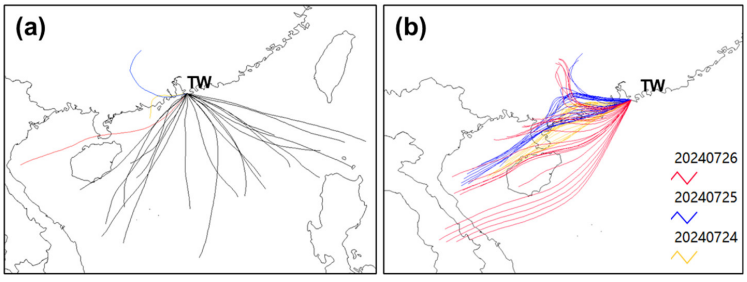

Figure 4. Back-trajectory analysis for air masses arriving at the TW site during the summer 2024 cruise campaign. (a) 24-h backward trajectories for the entire sampling period from 12 July to 3 August 2024. (b) 1-h backward trajectories during the typhoon-affected period from 24 to 26 July 2024, highlighting southwest and northwest transport pathways.

Overall, ON exhibited relatively weak temporal variability compared to IN throughout the campaign, suggesting that bulk ON concentrations were governed largely by regional-scale sources and atmospheric mixing. Nevertheless, episodic enhancements (e.g., 14 July) indicate that ON can still respond to favorable photochemical conditions associated with elevated ozone oxidation capacity. Although bulk ON concentrations in marine and urban $PM_{2.5}$ are broadly comparable, their underlying composition may differ substantially, particularly in the relative contributions of oxidized versus reduced nitrogen functionalities. This compositional contrast is examined using molecular-level analysis in the following section.

3.3 From oxidized to reduced nitrogen: molecular fragments for contrasting ON chemistry

ON in atmospheric fine particles represents a chemically diverse pool that integrates contributions from primary emissions, secondary formation, and multiphase processing. Its oxidation state provides critical information on both sources and atmospheric transformation pathways. In coastal megacity regions, ON chemistry is further complicated by the coexistence of intense anthropogenic emissions, marine

https://doi.org/10.5194/egusphere-2026-3750
Preprint. Discussion started: 7 July 2026

biogenic inputs, and strong air–sea interactions, leading to substantial variability in the relative importance of oxidized versus reduced nitrogen species. Here, we investigate the molecular evidence for contrasting ON chemistry in marine, urban, and ship-emission-influenced aerosols, with particular emphasis on how anthropogenic influence and marine boundary layer processing modulate the distribution of oxidized and reduced nitrogen species.

3.3.1 Reduced vs. oxidized ON in marine and urban aerosols

Our offline AMS results (Fig. 5a) show a substantially greater contribution of CHN-only formula classes (compounds containing C, H, and N but no O) in marine samples than in urban samples, particularly for fragments with one N atom (CHN1) (Fig. 5a, S5a). These CHN species, which include protonated amines and related bases, are consistent with an abundance of reduced ON compounds in the marine boundary layer (Mattsson et al., 2025), in line with previous reports that marine aerosol ON is enriched in reduced nitrogen species of marine biogenic origin, such as alkyl amines and amino acids (Calderón et al., 2007; Wedyan and Preston, 2008). In remote marine aerosols, most ON derives from biological production in the surface ocean (e.g., plankton exudates) rather than from continental pollution, and water-soluble ON correlates with ocean productivity and wind speed, implicating bubble-burst ejection of dissolved organic matter as a primary source (Altieri et al., 2016). Gaseous amines emitted from the ocean readily partition into acidic marine aerosol as ammonium salts (Ge et al., 2011). Urban aerosol ON, by contrast, shows a lower fraction of CHN-only formulas and a higher proportion of oxygenated organonitrogen formulas (CHON classes), reflecting oxidized nitrogen functionality (e.g., organic nitrates, nitro-aromatic compounds) formed via photochemistry (Zhu et al., 2025). We note that the CHON category includes compounds like amides or amino acid derivatives, so it is not a pure proxy for highly oxidized ON.

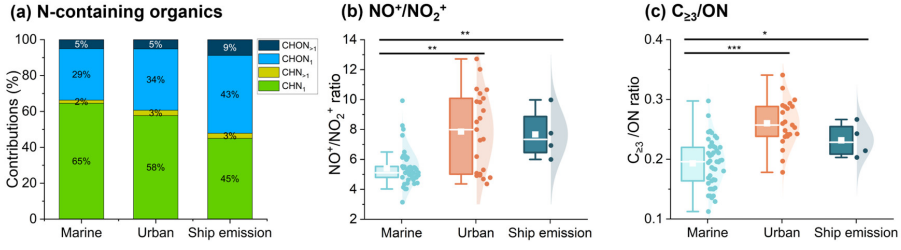

Figure 5. Comparison of N-containing organic fragments and related ratios in marine, urban, and ship-emission-influenced $PM_{2.5}$ samples. (a) Relative contributions of CHN_1, $CHN_{>1}$, $CHON_1$, and $CHON_{>1}$ formula classes to total organic N-containing fragments. (b) NO^+/NO_2^+ ratio, used as an indicator of oxidized nitrogen. (c) Ratio of N-containing organic fragments with carbon number ≥3 to total N-containing organic fragments ($C_{\geq 3}$/ON). Asterisks indicate statistically significant differences based on the one-sided Mann–Whitney–Wilcoxon test (* p<0.05, ** p<0.01, *** p<0.001). Additional Mann–Whitney–Wilcoxon test results were summarized in Table S4.

The NO^+/NO_2^+ ratio from offline AMS spectra provides a more direct measure of organic-nitrate character. Urban aerosols show significantly higher ratios (7.9 ± 2.6) than marine samples (5.3 ± 1.3) (Fig. 5b), indicating a greater contribution from oxidized ON species. This is supported by concurrent

https://doi.org/10.5194/egusphere-2026-3750
Preprint. Discussion started: 7 July 2026

NO_x observations (Fig. S6), which show generally higher NO_x at the Tsuen Wan urban site than in marine air, providing a more NO_x-rich environment for VOC oxidation and secondary organic nitrate formation—consistent with recent field studies linking high-NO_x conditions to enhanced particulate organic nitrate (Zhu et al., 2025; Graeffe et al., 2023). Importantly, molecular marker fragments provide direct corroborating evidence: clear signals at m/z 75 ($CHNO_3^+$) and 76 ($CH_2NO_3^+$), previously reported as characteristic organic-nitrate fragments (Fry et al., 2011), are observed in the urban spectra (Fig. S5b) and exhibit strong co-variation (Fig. S7b), suggesting a common organic-nitrate sub-mixture (shared precursors and/or fragmentation pathways). In marine samples, both their abundance and co-variation are much weaker (Fig. S7a), confirming a substantially larger and more coherent urban contribution from organic-nitrate-related ON chemistry.

A further structural constraint comes from the ratio of C≥3 N-containing organic fragments to total N-containing organic fragments (Fig. 5c), which is higher in urban samples. Interpreted conservatively, this points to an increased contribution of ON components with larger carbon backbones and/or greater molecular complexity. Such a pattern is consistent with the stronger influence of fossil-fuel and traffic-related combustion in urban air, which directly emits carbon-rich N-containing organics (e.g., nitro-PAHs and related N-aromatic species) (Kostenidou et al., 2021), as well as cooking emissions (alkanes, fatty acids, etc.) (Abdullahi et al., 2013) that supply precursors for subsequent oxidative processing. Together, these lines of evidence indicate that marine ON is dominated by reduced, biogenic nitrogen compounds, whereas urban ON is shifted toward oxidized, carbon-rich secondary organonitrogen species (Zhu et al., 2025).

3.3.2 Unique ON chemistry in ship-emission-influenced aerosols

Aerosols influenced by ship emissions show an interesting blend of these characteristics. In our ship-impacted samples (marine air masses intermittently under a shipping corridor), the NO^+/NO_2^+ ratio (7.7 ± 1.7) was higher than that of marine samples (Fig. 5b), highlighting substantial formation of oxidized ON, likely due to abundant ship-derived NO_x promoting organic nitrate production (Chen et al., 2024). The average N-containing fragment spectrum also shows enhanced oxygenated organonitrogen contributions relative to the marine case (Fig. S5c), indicating that oxidized ON chemistry is amplified when marine air masses are intermittently impacted by shipping.

At the same time, ship-influenced samples retain signatures consistent with reduced-N chemistry (Fig. 5a, S5c), suggesting that marine-background reduced nitrogen (e.g., NH_3, amines) can coexist with ship-derived oxidants and organic precursors. This co-existence provides a plausible environment for multiphase reactions producing N-containing organics beyond simple nitrate functionality. These aerosols also had elevated contributions of $CHON_1$-type formulas and showed distinctive mass spectral markers for imidazole-like heterocycles and amides. For example, fragments with two nitrogen atoms ($C_xH_yN_2^+$), indicative of imidazole-like ring structures, were enhanced in ship-influenced aerosol (Fig. S8). Such imidazole-like heterocycle formation can occur via aqueous-phase reactions of carbonyl

https://doi.org/10.5194/egusphere-2026-3750
Preprint. Discussion started: 7 July 2026

oxidation products (e.g., glyoxal, methylglyoxal) with ammonia or amines in particles (Yang et al., 2023). We propose that in ship-plume conditions, high NO_x and organic vapors from fuel combustion generate oxidized intermediates (organic nitrates, carbonyls) while co-emitted or marine-background NH_3/amines partake in multiphase reactions, producing secondary amides and imidazole-like heterocycles (including brown carbon species). Such pathways offer a mechanistic explanation for why ship-influenced aerosols can display both elevated oxidized-N indicators and distinctive reduced-N-derived organic signatures. Ship emissions supply NO_x and reactive organic precursors, while the marine boundary layer provides reduced nitrogen and aqueous processing environments that favor secondary formation of N-containing organics.

3.4 $PM_{2.5}$-bound nitrogen dry deposition

We estimated $PM_{2.5}$-bound N dry deposition fluxes using the inferential method (Eq. 1), combining measured ambient concentrations with literature-constrained dry deposition velocities (V_d). Since V_d for fine particles is sensitive to wind speed, surface roughness, particle size, and atmospheric stability (Zhang et al., 2001; Zhang et al., 2012; Farmer et al., 2021), the determination of V_d should account for the contrasting meteorological and surface conditions between the marine and coastal urban environments. In this study, shipboard meteorological measurements were available during the cruise campaign and showed that wind speeds over the marine region were substantially higher than those at the nearby Shell Tsing Yi station (SHL), which is located approximately 3 km from the Tsuen Wan urban sampling site and is used here to represent the coastal urban wind environment. Specifically, concurrent wind observations indicate substantially stronger winds over the GBA ocean (~5.5 m s^{-1}) than over the station near Tsuen Wan (SHL) (~2.6 m s^{-1}) (Fig. S9). This contrast indicates stronger wind-driven turbulent exchange over the marine region, although deposition to the smoother water surface may be less efficient than deposition to rougher built surfaces.

To constrain representative V_d values, we conducted a first-order calculation following the size-segregated particle dry-deposition scheme of Zhang et al. (2001), as described in the Supplement, where the governing equations, input parameters (Table S1), and calculated intermediate and final results (Table S2) are summarized. The calculated V_d values were 0.11 cm s^{-1} for the marine environment and 0.13 cm s^{-1} for the coastal urban environment (Table 2). The slightly higher urban V_d, despite the lower urban wind speed, reflects the larger urban roughness length and lower aerodynamic resistance in the Zhang et al. (2001) framework, while the stronger marine winds partly offset the smoother water surface. The calculated V_d values are comparable to previous reported fine-particle V_d observations and estimates (Wu et al., 2018; Pryor et al., 2008; Farmer et al., 2021).

Applying these estimated V_d values to the measured $PM_{2.5}$ nitrogen components, the annual dry deposition fluxes of $PM_{2.5}$-bound TN were estimated to be 0.14 kg N ha^{-1} yr^{-1} over the marine region and 0.15 kg N ha^{-1} yr^{-1} at the coastal urban site (Table 2). These results indicate that fine-particle N dry deposition over the GBA coastal waters was of the same order as that at the adjacent coastal urban site.

https://doi.org/10.5194/egusphere-2026-3750
Preprint. Discussion started: 7 July 2026

This result highlights that nearshore marine N deposition should not be regarded as a simple diluted extension of urban deposition. Instead, the coastal ocean can receive non-negligible fine-particle N inputs because marine aerosol N concentrations remain appreciable. Thus, fine-particle N deposition over the GBA coastal ocean may represent an important atmospheric input pathway that should not be overlooked when assessing regional N budgets and potential ecosystem responses.

Table 2. Representative V_d and estimated $PM_{2.5}$-bound TN dry deposition fluxes for the marine region and the coastal urban site.

Environment	V_d (cm s^{-1})	N dry deposition (kg N ha^{-1} yr^{-1})	Interpretation
Marine region	0.11	0.14	Calculated using the observed shipboard wind speed and an open-water roughness assumption; stronger marine winds partly offset the smoother water surface.
Coastal urban site	0.13	0.15	Calculated using the lower urban reference wind speed but larger urban roughness length, which reduces aerodynamic resistance over built surfaces.

It is important to emphasize that the present estimates represent only the fine-particle ($PM_{2.5}$-bound) nitrogen contribution to dry deposition, however, the coarse-mode particulate nitrogen and gas-phase reactive nitrogen species were not included. Previous measurements in urban Hong Kong indicate that coarse particulate N deposition can exceed fine-mode deposition by roughly a factor of two (e.g., 0.77 vs. 1.42 kg N ha^{-1} yr^{-1} for fine and coarse fractions, respectively) (Yu et al., 2023). In addition, water-soluble gaseous species such as NH_3, HNO_3, and organic nitrogen vapors may also contribute significantly to total dry nitrogen deposition (Jia et al., 2016). Consequently, the fluxes estimated in this study based only on $PM_{2.5}$ are expected to be substantially lower than total dry nitrogen deposition values reported in many other studies, which often encompass these additional components. For example, dry deposition of N in urban Guangzhou has been reported to reach 13.7 kg N ha^{-1} yr^{-1} (Yu et al., 2020), while values of 5.9 kg N ha^{-1} yr^{-1} have been reported for Singapore (He et al., 2011). In Europe, coastal measurements indicate N dry deposition fluxes of approximately 5.0 kg N ha^{-1} yr^{-1} in Edinburgh, UK (González Benítez et al., 2009), and 5.9 kg N ha^{-1} yr^{-1} at Finokalia in the eastern Mediterranean (Violaki et al., 2010). Taken together, these results suggest that the GBA coastal atmosphere is characterized by a sharp land–sea transition in both $PM_{2.5}$ nitrogen abundance and chemical form, with more oxidized ON signatures in the coastal urban environment and a greater relative contribution of reduced ON species in the marine boundary layer. A conceptual summary of the contrasting nitrogen chemistry, atmospheric deposition pathway, and potential ecosystem implications is shown in Fig. 6.

https://doi.org/10.5194/egusphere-2026-3750
Preprint. Discussion started: 7 July 2026

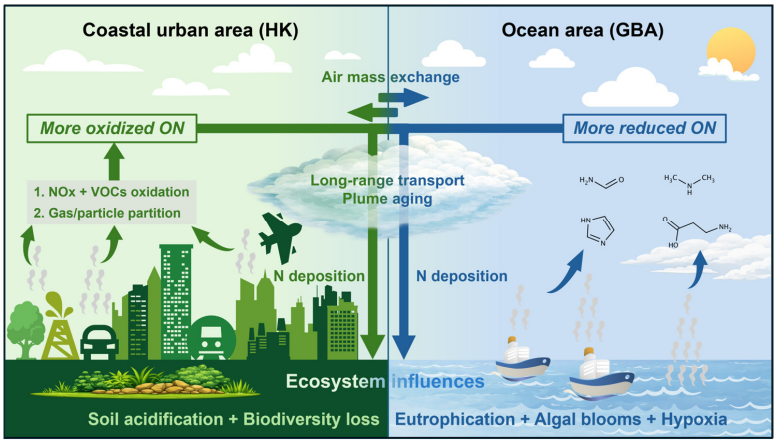

Figure 6. Conceptual summary of aerosol nitrogen chemistry, deposition pathways, and potential ecosystem implications in the coastal GBA atmosphere.

4. Conclusions and implications

This study presents the first paired marine–urban characterization of $PM_{2.5}$-bound TN, IN, and ON in the GBA, based on sampling at a coastal urban site (Tsuen Wan) and concurrent shipboard sampling over the adjacent coastal waters. We show that the coastal marine atmosphere of the GBA is not simply a diluted extension of the urban atmosphere but has a distinct nitrogen chemical signature shaped by both regional transport and marine boundary-layer processing. This helps address a long-standing uncertainty in coastal nitrogen deposition studies: the limited chemical characterization of ON in marine aerosols.

Three principal findings emerge. First, TN and IN increased from west to east across the GBA coastal waters and decreased offshore, while ON exhibited a much stronger and more coherent offshore gradient than IN, and the ON/TN fraction peaked in the more marine-influenced western region (~35%), indicating that ON remains an important component of aerosol N under lower particle loadings. Second, although bulk IN and ON concentrations were broadly comparable between marine and urban $PM_{2.5}$, their underlying chemistry differed sharply: urban aerosols were strongly NH_4^+-dominated ($N\text{–}NH_4^+/N\text{–}NO_3^- \approx 5.4$) with higher NO^+/NO_2^+ ratios (7.9 ± 2.6), larger CHON contributions, clear organic-nitrate marker fragments (*m/z* 75, 76), and a higher fractional abundance of $C_{\geq 3}$ ON fragments, all consistent with NO_x–VOC photochemistry; whereas marine aerosols were more enriched in CHN-type reduced-N fragments (e.g., amines), retained appreciable nitrate consistent with sea-salt processing, and showed lower NO^+/NO_2^+ ratios (5.3 ± 1.3). Ship-emission-influenced samples displayed a hybrid signature, combining elevated oxidized-N indicators with distinctive reduced-N-related markers (e.g., imidazole-like $C_xH_yN_2^+$ fragments). Third, $PM_{2.5}$-bound N deposition was estimated at 0.14 kg N ha^{-1} yr^{-1} over the marine region and 0.15 kg N ha^{-1} yr^{-1} at the urban site; nearshore marine deposition was of the same order as that at the coastal urban site.

https://doi.org/10.5194/egusphere-2026-3750
Preprint. Discussion started: 7 July 2026

These findings have several implications beyond deposition magnitude alone.

Implications for model representation of atmospheric N speciation in coastal megacity regions. The contrasting marine–urban nitrogen chemistry documented here demonstrates that the chemical form of aerosol N transitions notably across the land–sea interface, even when bulk concentrations are similar. This has direct consequences for source apportionment and chemical transport modeling in coastal megacity systems: representing $PM_{2.5}$ N as a single bulk pool, or applying urban-derived ON source profiles to adjacent marine grid cells, will misrepresent both the oxidation state and the likely sources of N over the coastal ocean. Our results indicate that coupled urban–marine modeling of the GBA should explicitly resolve (a) NO_x–VOC-driven oxidized-ON formation in the urban plume, (b) NH_3/amine partitioning and reduced-ON enrichment in the marine boundary layer, and (c) the multiphase chemistry that arises when ship-emitted NO_x interacts with marine reduced nitrogen to generate secondary amides, imidazole-like heterocycles, and other N-containing organics.

Implications for marine ecosystem responses. The chemical form of deposited N determines its bioavailability and its biogeochemical fate. Our $PM_{2.5}$ composition indicates a stronger contribution of reduced N (NH_x and reduced ON) in the marine boundary layer, which is particularly important because NH_4^+ is readily assimilable and often energetically favored over NO_3^- for phytoplankton uptake. In the South China Sea, atmospheric N deposition has been shown to support on the order of ~20% of annual new production in some assessments (Kim et al., 2014), and episodic aerosol nutrient inputs can shift nutrient limitation (e.g., increasing N:P) and promote bloom-favorable conditions in coastal–shelf waters (Mackey et al., 2017; Guo et al., 2022). The reduced-N enrichment we observe in nearshore marine $PM_{2.5}$, combined with the non-negligible deposition fluxes estimated using representative V_d values, suggests that fine-particle reduced-N inputs along the GBA coast could measurably strengthen bioavailable N supply, perturb C:N:P stoichiometry, and contribute to eutrophication and HAB-prone conditions documented in the northern South China Sea (He et al., 2023). The distinctive ship-influenced ON chemistry (oxidized-N indicators co-occurring with imidazole-like and amide-like markers) further suggests that shipping corridors are not only NO_x sources but also sites where chemically complex, potentially light-absorbing N-containing organic aerosol is generated, with downstream implications for both deposition speciation and marine boundary-layer radiative properties that warrant further study. It should be noted that these implications may be particularly relevant for the eastern GBA coastal waters, including Mirs Bay, corresponding to region C (Fig. 2a), where summer waters are less affected by the nutrient-rich Pearl River discharge and have relatively low nutrient concentrations (Li et al., 2020; Lo et al., 2025). Under such lower-nutrient conditions, anthropogenically influenced aerosol ON and reduced-N inputs from the atmosphere may play an important role in bioavailable N supply and local ocean productivity in this region.

Implications for nitrogen deposition budgets and management. Two practical points follow from the deposition analysis. First, because the present estimates include only the $PM_{2.5}$ fraction and exclude coarse-mode particles, gas-phase reactive nitrogen (NH_3, HNO_3, organic N vapors), and wet deposition,

https://doi.org/10.5194/egusphere-2026-3750
Preprint. Discussion started: 7 July 2026

they represent a lower bound on total atmospheric N input to the GBA coastal ocean; comparison with previous regional studies (e.g., 13.7 kg N ha^{-1} yr^{-1} in urban Guangzhou; 5.9 kg N ha^{-1} yr^{-1} in Singapore) underscores how substantial the missing components are likely to be. Closing this budget for the GBA coastal zone will require future paired marine–urban campaigns that extend the present framework to total suspended particles, gas-phase species, and wet deposition. Second, the marine–urban contrast in nitrogen form has direct relevance for coastal management: as continental NO_x emissions continue to decline across southern China while NH_3 emissions remain high, the relative importance of reduced-N (NH_x and reduced ON) deposition to coastal waters will likely increase. Integrating speciation-resolved atmospheric deposition constraints (rather than bulk-N fluxes) into chemical transport models coupled with coastal biogeochemical models would help diagnose ecosystem sensitivity to NH_x inputs specifically and explore thresholds relevant to eutrophication and HAB risk under changing emissions and meteorology.

Building on the limitations identified in this study, three priorities emerge as future research directions. First, the V_d uncertainty remains a major limitation of the deposition estimates and should be reduced through direct shipboard meteorological measurements (friction velocity, stability) during future cruises. Second, molecular-level identification and quantification of the specific reduced-ON species enriched in marine $PM_{2.5}$ (amines, amides, amino acids, imidazole-like heterocycles) would clarify their bioavailability and sources. Third, the unique ON chemistry observed in ship-emission-influenced samples merits dedicated investigation, given the GBA's role as one of the world's busiest shipping regions and the potential for ship plumes to act as distinct chemical reactors at the air–sea interface.

Data availability

Data used in this study are available upon request from the corresponding author.

Author contributions

C.C. and J.Z.Y. designed the research. C.C. collected the marine samples. C.C., W. Chen, W.H.M.W, N.S., and K.Z. conducted the sample analysis. C.C. and J.Z.Y. performed the data interpretation. C.C. wrote the paper. All authors contributed to the paper with useful scientific discussions.

Competing interests

The authors declare no competing interests.

https://doi.org/10.5194/egusphere-2026-3750
Preprint. Discussion started: 7 July 2026

Acknowledgements

This study was supported by the Center for Ocean Research in Hong Kong and Macau, a joint research centre for ocean research between Laoshan Laboratory and HKUST, and the Hong Kong Research Grants Council (AoE/P-601/23-N, CRS_HKUST605/24, and SRFS2526-6S05).

References

Abdullahi, K. L., Delgado-Saborit, J. M., and Harrison, R. M.: Emissions and indoor concentrations of particulate matter and its specific chemical components from cooking: A review, Atmospheric Environment, 71, 260-294, 10.1016/j.atmosenv.2013.01.061, 2013.

Altieri, K. E., Fawcett, S. E., Peters, A. J., Sigman, D. M., and Hastings, M. G.: Marine biogenic source of atmospheric organic nitrogen in the subtropical North Atlantic, Proc Natl Acad Sci U S A, 113, 925-930, 10.1073/pnas.1516847113, 2016.

Anderson, D. M., Glibert, P. M., and Burkholder, J. M.: Harmful algal blooms and eutrophication: Nutrient sources, composition, and consequences, Estuaries, 25, 704-726, 10.1007/BF02804901, 2002.

Bruns, E. A., Perraud, V., Zelenyuk, A., Ezell, M. J., Johnson, S. N., Yu, Y., Imre, D., Finlayson-Pitts, B. J., and Alexander, M. L.: Comparison of FTIR and Particle Mass Spectrometry for the Measurement of Particulate Organic Nitrates, Environ. Sci. Technol., 44, 1056-1061, 10.1021/es9029864, 2010.

Calderón, S. M., Poor, N. D., and Campbell, S. W.: Estimation of the particle and gas scavenging contributions to wet deposition of organic nitrogen, Atmospheric Environment, 41, 4281-4290, https://doi.org/10.1016/j.atmosenv.2006.06.067, 2007.

Cape, J. N., Cornell, S. E., Jickells, T. D., and Nemitz, E.: Organic nitrogen in the atmosphere — Where does it come from? A review of sources and methods, Atmospheric Research, 102, 30-48, 10.1016/j.atmosres.2011.07.009, 2011.

Chen, J., Fu, X., Wang, X., Dong, S., Chen, T., Xue, L., Zhou, Y., Sheng, L., and Wang, W.: Unveiling the overlooked direct emissions of particulate organic nitrates from ship, Environment International, 185, 108487, https://doi.org/10.1016/j.envint.2024.108487, 2024.

Chow, W. S., Liao, K., Huang, X. H. H., Leung, K. F., Lau, A. K. H., and Yu, J. Z.: Measurement report: The 10-year trend of $PM_{2.5}$ major components and source tracers from 2008 to 2017 in an urban site of Hong Kong, China, Atmospheric Chemistry and Physics, 22, 11557-11577, 10.5194/acp-22-11557-2022, 2022.

Daellenbach, K. R., Bozzetti, C., Křepelová, A., Canonaco, F., Wolf, R., Zotter, P., Fermo, P., Crippa, M., Slowik, J. G., Sosedova, Y., Zhang, Y., Huang, R. J., Poulain, L., Szidat, S., Baltensperger, U., El Haddad, I., and Prévôt, A. S. H.: Characterization and source apportionment of organic aerosol using offline aerosol mass spectrometry, Atmospheric Measurement Techniques, 9, 23-39, 10.5194/amt-9-23-2016, 2016.

Davies, J. A. and Cox, R. A.: Kinetics of the Heterogeneous Reaction of HNO_3 with NaCl: Effect of Water Vapor, The Journal of Physical Chemistry A, 102, 7631-7642, 10.1021/jp982134t, 1998.

DeCarlo, P. F., Kimmel, J. R., Trimborn, A., Northway, M. J., Jayne, J. T., Aiken, A. C., Gonin, M., Fuhrer, K., Horvath, T., Docherty, K. S., Worsnop, D. R., and Jimenez, J. L.: Field-Deployable, High-Resolution, Time-of-Flight Aerosol Mass Spectrometer, Analytical Chemistry, 78, 8281-8289, 10.1021/ac061249n, 2006.

https://doi.org/10.5194/egusphere-2026-3750
Preprint. Discussion started: 7 July 2026

634 Diaz, R. J. and Rosenberg, R.: Spreading Dead Zones and Consequences for Marine Ecosystems, Science, 321,
635 926-929, 10.1126/science.1156401, 2008.
636 Duce, R. A., LaRoche, J., Altieri, K., Arrigo, K. R., Baker, A. R., Capone, D. G., Cornell, S., Dentener, F.,
637 Galloway, J., Ganeshram, R. S., Geider, R. J., Jickells, T., Kuypers, M. M., Langlois, R., Liss, P. S., Liu, S. M.,
638 Middelburg, J. J., Moore, C. M., Nickovic, S., Oschlies, A., Pedersen, T., Prospero, J., Schlitzer, R., Seitzinger,
639 S., Sorensen, L. L., Uematsu, M., Ulloa, O., Voss, M., Ward, B., and Zamora, L.: Impacts of Atmospheric
640 Anthropogenic Nitrogen on the Open Ocean, Science, 320, 893-897, 10.1126/science.1150369, 2008.
641 Farmer, D. K., Boedicker, E. K., and DeBolt, H. M.: Dry Deposition of Atmospheric Aerosols: Approaches,
642 Observations, and Mechanisms, Annu Rev Phys Chem, 72, 375-397, 10.1146/annurev-physchem-090519-
643 034936, 2021.
644 Farmer, D. K., Matsunaga, A., Docherty, K. S., Surratt, J. D., Seinfeld, J. H., Ziemann, P. J., and Jimenez, J. L.:
645 Response of an aerosol mass spectrometer to organonitrates and organosulfates and implications for atmospheric
646 chemistry, Proceedings of the National Academy of Sciences, 107, 6670-6675, 10.1073/pnas.0912340107, 2010.
647 Fry, J. L., Kiendler-Scharr, A., Rollins, A. W., Wooldridge, P. J., Brown, S. S., Fuchs, H., Dubé, W., Mensah, A.,
648 dal Maso, M., Tillmann, R., Dorn, H. P., Brauers, T., and Cohen, R. C.: Organic nitrate and secondary organic
649 aerosol yield from NO_3 oxidation of β-pinene evaluated using a gas-phase kinetics/aerosol partitioning model,
650 Atmos. Chem. Phys., 9, 1431-1449, 10.5194/acp-9-1431-2009, 2009.
651 Fry, J. L., Kiendler-Scharr, A., Rollins, A. W., Brauers, T., Brown, S. S., Dorn, H. P., Dubé, W. P., Fuchs, H.,
652 Mensah, A., Rohrer, F., Tillmann, R., Wahner, A., Wooldridge, P. J., and Cohen, R. C.: SOA from limonene: role
653 of NO_3 in its generation and degradation, Atmospheric Chemistry and Physics, 11, 3879-3894, 10.5194/acp-11-
654 3879-2011, 2011.
655 Galloway, J. N., Townsend, A. R., Erisman, J. W., Bekunda, M., Cai, Z., Freney, J. R., Martinelli, L. A.,
656 Seitzinger, S. P., and Sutton, M. A.: Transformation of the Nitrogen Cycle: Recent Trends, Questions, and
657 Potential Solutions, Science, 320, 889-892, 10.1126/science.1136674, 2008.
658 Ge, X., Wexler, A. S., and Clegg, S. L.: Atmospheric amines – Part II. Thermodynamic properties and gas/particle
659 partitioning, Atmospheric Environment, 45, 561-577, https://doi.org/10.1016/j.atmosenv.2010.10.013, 2011.
660 Ge, X., Sun, Y., Trousdell, J., Chen, M., and Zhang, Q.: Enhancing characterization of organic nitrogen
661 components in aerosols and droplets using high-resolution aerosol mass spectrometry, Atmospheric Measurement
662 Techniques, 17, 423-439, 10.5194/amt-17-423-2024, 2024.
663 González Benítez, J. M., Cape, J. N., Heal, M. R., van Dijk, N., and Díez, A. V.: Atmospheric nitrogen deposition
664 in south-east Scotland: Quantification of the organic nitrogen fraction in wet, dry and bulk deposition,
665 Atmospheric Environment, 43, 4087-4094, 10.1016/j.atmosenv.2009.04.061, 2009.
666 Graeffe, F., Heikkinen, L., Garmash, O., Aijala, M., Allan, J., Feron, A., Cirtog, M., Petit, J. E., Bonnaire, N.,
667 Lambe, A., Favez, O., Albinet, A., Williams, L. R., and Ehn, M.: Detecting and Characterizing Particulate Organic
668 Nitrates with an Aerodyne Long-ToF Aerosol Mass Spectrometer, ACS Earth Space Chem, 7, 230-242,
669 10.1021/acsearthspacechem.2c00314, 2023.
670 Guimbaud, C., Arens, F., Gutzwiller, L., Gäggeler, H. W., and Ammann, M.: Uptake of HNO_3 to deliquescent
671 sea-salt particles: a study using the short-lived radioactive isotope tracer ^{13}N, Atmos. Chem. Phys., 2, 249-257,
672 10.5194/acp-2-249-2002, 2002.

https://doi.org/10.5194/egusphere-2026-3750
Preprint. Discussion started: 7 July 2026

673 Guo, C., Zhou, Y., Zhou, H., Su, C., and Kong, L.: Aerosol Nutrients and Their Biological Influence on the
674 Northwest Pacific Ocean (NWPO) and Its Marginal Seas, Biology (Basel), 11, 10.3390/biology11060842, 2022.
675 He, J., Balasubramanian, R., Burger, D. F., Hicks, K., Kuylenstierna, J. C. I., and Palani, S.: Dry and wet
676 atmospheric deposition of nitrogen and phosphorus in Singapore, Atmospheric Environment, 45, 2760-2768,
677 10.1016/j.atmosenv.2011.02.036, 2011.
678 He, W., Lai, Z., Lu, W., Li, D., and Chen, C.: The Effects of Atmospheric Nitrogen Deposition on the Marine
679 Ecosystem of the Northern South China Sea, Journal of Geophysical Research: Oceans, 128, e2022JC018790,
680 https://doi.org/10.1029/2022JC018790, 2023.
681 Howarth, R. W. and Marino, R.: Nitrogen as the limiting nutrient for eutrophication in coastal marine ecosystems:
682 Evolving views over three decades, Limnology and Oceanography, 51, 364-376,
683 https://doi.org/10.4319/lo.2006.51.1_part_2.0364, 2006.
684 Hui, E. C. M., Li, X., Chen, T., and Lang, W.: Deciphering the spatial structure of China's megacity region: A
685 new bay area—The Guangdong-Hong Kong-Macao Greater Bay Area in the making, Cities, 105,
686 10.1016/j.cities.2018.10.011, 2020.
687 Jia, Y., Yu, G., Gao, Y., He, N., Wang, Q., Jiao, C., and Zuo, Y.: Global inorganic nitrogen dry deposition inferred
688 from ground- and space-based measurements, Sci Rep, 6, 19810, 10.1038/srep19810, 2016.
689 Jickells, T., Baker, A. R., Cape, J. N., Cornell, S. E., and Nemitz, E.: The cycling of organic nitrogen through the
690 atmosphere, Philos Trans R Soc Lond B Biol Sci, 368, 20130115, 10.1098/rstb.2013.0115, 2013.
691 Kanakidou, M., Myriokefalitakis, S., Daskalakis, N., Fanourgakis, G., Nenes, A., Baker, A. R., Tsigaridis, K., and
692 Mihalopoulos, N.: Past, Present and Future Atmospheric Nitrogen Deposition, J Atmos Sci, 73, 2039-2047,
693 10.1175/JAS-D-15-0278.1, 2016.
694 Kanakidou, M., Duce, R. A., Prospero, J. M., Baker, A. R., Benitez-Nelson, C., Dentener, F. J., Hunter, K. A.,
695 Liss, P. S., Mahowald, N., Okin, G. S., Sarin, M., Tsigaridis, K., Uematsu, M., Zamora, L. M., and Zhu, T.:
696 Atmospheric fluxes of organic N and P to the global ocean, Global Biogeochemical Cycles, 26,
697 10.1029/2011gb004277, 2012.
698 Kim, T.-W., Lee, K., Duce, R., and Liss, P.: Impact of atmospheric nitrogen deposition on phytoplankton
699 productivity in the South China Sea, Geophysical Research Letters, 41, 3156-3162,
700 https://doi.org/10.1002/2014GL059665, 2014.
701 Kostenidou, E., Martinez-Valiente, A., R'Mili, B., Marques, B., Temime-Roussel, B., Durand, A., André, M., Liu,
702 Y., Louis, C., Vansevenant, B., Ferry, D., Laffon, C., Parent, P., and D'Anna, B.: Technical note: Emission factors,
703 chemical composition, and morphology of particles emitted from Euro 5 diesel and gasoline light-duty vehicles
704 during transient cycles, Atmospheric Chemistry and Physics, 21, 4779-4796, 10.5194/acp-21-4779-2021, 2021.
705 Lee, M., Shevliakova, E., Stock, C. A., Malyshev, S., and Milly, P. C. D.: Prominence of the tropics in the recent
706 rise of global nitrogen pollution, Nat Commun, 10, 1437, 10.1038/s41467-019-09468-4, 2019.
707 Li, D., Gan, J., Hui, R., Liu, Z., Yu, L., Lu, Z., and Dai, M.: Vortex and Biogeochemical Dynamics for the Hypoxia
708 Formation Within the Coastal Transition Zone off the Pearl River Estuary, Journal of Geophysical Research:
709 Oceans, 125, 10.1029/2020jc016178, 2020.
710 Lo, H. W., Yu, X., Chen, H., Chu, W. C., Chung, N. M., Lau, S. W., Li, J., Liang, S., Liao, K., Thomas, H. C. J.,
711 Wang, Z., Zhang, Z., Yu, J. Z., and Thibodeau, B.: Tidal currents and atmospheric inorganic nitrogen contribute

https://doi.org/10.5194/egusphere-2026-3750
Preprint. Discussion started: 7 July 2026

to diurnal variation of dissolved nutrients and chlorophyll a concentrations in Mirs Bay, Hong Kong, Regional Studies in Marine Science, 81, 103941, https://doi.org/10.1016/j.rsma.2024.103941, 2025.

Luo, L., Kao, S.-J., Bao, H., Xiao, H., Xiao, H., Yao, X., Gao, H., Li, J., and Lu, Y.: Sources of reactive nitrogen in marine aerosol over the Northwest Pacific Ocean in spring, Atmospheric Chemistry and Physics, 18, 6207-6222, 10.5194/acp-18-6207-2018, 2018.

Mackey, K. R. M., Kavanaugh, M. T., Wang, F., Chen, Y., Liu, F., Glover, D. M., Chien, C.-T., and Paytan, A.: Atmospheric and Fluvial Nutrients Fuel Algal Blooms in the East China Sea, Frontiers in Marine Science, Volume 4 - 2017, 10.3389/fmars.2017.00002, 2017.

Mahowald, N. M., Scanza, R., Brahney, J., Goodale, C. L., Hess, P. G., Moore, J. K., and Neff, J.: Aerosol Deposition Impacts on Land and Ocean Carbon Cycles, Current Climate Change Reports, 3, 16-31, 10.1007/s40641-017-0056-z, 2017.

Mattsson, F., Neuberger, A., Heikkinen, L., Gramlich, Y., Paglione, M., Rinaldi, M., Decesari, S., Zieger, P., Riipinen, I., and Mohr, C.: Enrichment of organic nitrogen in fog residuals observed in the Italian Po Valley, Atmospheric Chemistry and Physics, 25, 7973-7989, 10.5194/acp-25-7973-2025, 2025.

Ng, N. L., Brown, S. S., Archibald, A. T., Atlas, E., Cohen, R. C., Crowley, J. N., Day, D. A., Donahue, N. M., Fry, J. L., Fuchs, H., Griffin, R. J., Guzman, M. I., Herrmann, H., Hodzic, A., Iinuma, Y., Jimenez, J. L., Kiendler-Scharr, A., Lee, B. H., Luecken, D. J., Mao, J., McLaren, R., Mutzel, A., Osthoff, H. D., Ouyang, B., Picquet-Varrault, B., Platt, U., Pye, H. O. T., Rudich, Y., Schwantes, R. H., Shiraiwa, M., Stutz, J., Thornton, J. A., Tilgner, A., Williams, B. J., and Zaveri, R. A.: Nitrate radicals and biogenic volatile organic compounds: oxidation, mechanisms, and organic aerosol, Atmos Chem Phys, 17, 2103-2162, 10.5194/acp-17-2103-2017, 2017.

Nie, W., Yan, C., Huang, D. D., Wang, Z., Liu, Y., Qiao, X., Guo, Y., Tian, L., Zheng, P., Xu, Z., Li, Y., Xu, Z., Qi, X., Sun, P., Wang, J., Zheng, F., Li, X., Yin, R., Dallenbach, K. R., Bianchi, F., Petäjä, T., Zhang, Y., Wang, M., Schervish, M., Wang, S., Qiao, L., Wang, Q., Zhou, M., Wang, H., Yu, C., Yao, D., Guo, H., Ye, P., Lee, S., Li, Y. J., Liu, Y., Chi, X., Kerminen, V.-M., Ehn, M., Donahue, N. M., Wang, T., Huang, C., Kulmala, M., Worsnop, D., Jiang, J., and Ding, A.: Secondary organic aerosol formed by condensing anthropogenic vapours over China's megacities, Nature Geoscience, 15, 255-261, 10.1038/s41561-022-00922-5, 2022.

Nuruddin, M. F., Poon, Y. C. J., He, X., Zhang, Z., Tang, X., Lee, S. S., Zhang, S., He, D., and Wu, L.: Zooplankton Metabolism Shapes Molecular Composition of Dissolved Organic Matter in Coastal Waters, Environ. Sci. Technol., 10.1021/acs.est.6c05592, 2026.

Palta, M. M. and Hartnett, H. E.: Nitrogen Cycle, in: Encyclopedia of Geochemistry: A Comprehensive Reference Source on the Chemistry of the Earth, edited by: White, W. M., Springer International Publishing, Cham, 987-991, 10.1007/978-3-319-39312-4_160, 2018.

Park, J. and Song, H.: Variance of destination region image according to multi-dimensional proximity: A case of the Greater Bay Area, Journal of Destination Marketing & Management, 20, 10.1016/j.jdmm.2021.100600, 2021.

Paulot, F., Jacob, D. J., Johnson, M. T., Bell, T. G., Baker, A. R., Keene, W. C., Lima, I. D., Doney, S. C., and Stock, C. A.: Global oceanic emission of ammonia: Constraints from seawater and atmospheric observations, Global Biogeochemical Cycles, 29, 1165-1178, 10.1002/2015gb005106, 2015.

Pryor, S. C., Gallagher, M., Sievering, H., Larsen, S. E., Barthelmie, R. J., Birsan, F., Nemitz, E., Rinne, J., Kulmala, M., Grönholm, T., Taipale, R., and Vesala, T.: A review of measurement and modelling results of particle

https://doi.org/10.5194/egusphere-2026-3750
Preprint. Discussion started: 7 July 2026

752 atmosphere–surface exchange, Tellus B: Chemical and Physical Meteorology, 60, 10.1111/j.1600-
753 0889.2007.00298.x, 2008.
754 Seinfeld, J. H. and Pandis, S. N.: Atmospheric Chemistry and Physics: From Air Pollution to Climate Change,
755 2016.
756 Shi, J., Gao, H., Qi, J., Zhang, J., and Yao, X.: Sources, compositions, and distributions of water-soluble organic
757 nitrogen in aerosols over the China Sea, Journal of Geophysical Research: Atmospheres, 115,
758 10.1029/2009jd013238, 2010.
759 Violaki, K., Zarbas, P., and Mihalopoulos, N.: Long-term measurements of dissolved organic nitrogen (DON) in
760 atmospheric deposition in the Eastern Mediterranean: Fluxes, origin and biogeochemical implications, Marine
761 Chemistry, 120, 179-186, 10.1016/j.marchem.2009.08.004, 2010.
762 Vlachou, A., Daellenbach, K. R., Bozzetti, C., Chazeau, B., Salazar, G. A., Szidat, S., Jaffrezo, J.-L., Hueglin, C.,
763 Baltensperger, U., Haddad, I. E., and Prévôt, A. S. H.: Advanced source apportionment of carbonaceous aerosols
764 by coupling offline AMS and radiocarbon size-segregated measurements over a nearly 2-year period, Atmospheric
765 Chemistry and Physics, 18, 6187-6206, 10.5194/acp-18-6187-2018, 2018.
766 Wang, F., Shao, W., Yu, H., Kan, G., He, X., Zhang, D., Ren, M., and Wang, G.: Re-evaluation of the Power of
767 the Mann-Kendall Test for Detecting Monotonic Trends in Hydrometeorological Time Series, Frontiers in Earth
768 Science, 8, 10.3389/feart.2020.00014, 2020.
769 Wedyan, M. A. and Preston, M. R.: The coupling of surface seawater organic nitrogen and the marine aerosol as
770 inferred from enantiomer-specific amino acid analysis, Atmospheric Environment, 42, 8698-8705,
771 https://doi.org/10.1016/j.atmosenv.2008.04.038, 2008.
772 Wilcox, R.: Chapter 10 - Robust Regression, in: Introduction to Robust Estimation and Hypothesis Testing (Fourth
773 Edition), edited by: Wilcox, R., Academic Press, 517-583, https://doi.org/10.1016/B978-0-12-804733-0.00010-
774 X, 2017.
775 Wu, Y., Liu, J., Zhai, J., Cong, L., Wang, Y., Ma, W., Zhang, Z., and Li, C.: Comparison of dry and wet deposition
776 of particulate matter in near-surface waters during summer, PLoS One, 13, e0199241,
777 10.1371/journal.pone.0199241, 2018.
778 Yang, L., Huang, R.-J., Shen, J., Wang, T., Gong, Y., Yuan, W., Liu, Y., Huang, H., You, Q., Huang, D. D., and
779 Huang, C.: New Insights into the Brown Carbon Chromophores and Formation Pathways for Aqueous Reactions
780 of α-Dicarbonyls with Amines and Ammonium, Environ. Sci. Technol., 57, 12351-12361,
781 10.1021/acs.est.3c04133, 2023.
782 Yau, Y. Y., Baker, D. M., and Thibodeau, B.: Quantifying the Impact of Anthropogenic Atmospheric Nitrogen
783 Deposition on the Generation of Hypoxia under Future Emission Scenarios in Chinese Coastal Waters, Environ
784 Sci Technol, 54, 3920-3928, 10.1021/acs.est.0c00706, 2020.
785 Yu, X., Wong, Y. K., and Yu, J. Z.: Abundance and sources of organic nitrogen in fine ($PM_{2.5}$) and coarse ($PM_{2.5-10}$)
786 particulate matter in urban Hong Kong, Science of the Total Environment, 901, 165880,
787 10.1016/j.scitotenv.2023.165880, 2023.
788 Yu, X., Li, Q., Ge, Y., Li, Y., Liao, K., Huang, X. H., Li, J., and Yu, J. Z.: Simultaneous Determination of Aerosol
789 Inorganic and Organic Nitrogen by Thermal Evolution and Chemiluminescence Detection, Environ. Sci. Technol.,
790 55, 11579-11589, 10.1021/acs.est.1c04876, 2021.

https://doi.org/10.5194/egusphere-2026-3750
Preprint. Discussion started: 7 July 2026

Yu, X., Li, Q., Liao, K., Li, Y., Wang, X., Zhou, Y., Liang, Y., and Yu, J. Z.: New measurements reveal a large contribution of nitrogenous molecules to ambient organic aerosol, npj Climate and Atmospheric Science, 7, 10.1038/s41612-024-00620-6, 2024.

Yu, X., Pan, Y., Song, W., Li, S., Li, D., Zhu, M., Zhou, H., Zhang, Y., Li, D., Yu, J., Wang, X., and Wang, X.: Wet and Dry Nitrogen Depositions in the Pearl River Delta, South China: Observations at Three Typical Sites With an Emphasis on Water-Soluble Organic Nitrogen, Journal of Geophysical Research: Atmospheres, 125, 10.1029/2019jd030983, 2020.

Zhang, C., Wang, Y., Liu, J., Chen, T., Huang, W., Liu, Z., Chu, B., Ma, Q., and He, H.: Insight into wet scavenging effects on sulfur and nitrogen containing organic compounds in urban Beijing, npj Climate and Atmospheric Science, 7, 10.1038/s41612-024-00756-5, 2024a.

Zhang, J., Yu, L., Li, X., Zhang, C., Shi, T., Wu, X., Yang, C., Gao, W., Li, Q., and Wu, G.: Exploring Annual Urban Expansions in the Guangdong-Hong Kong-Macau Greater Bay Area: Spatiotemporal Features and Driving Factors in 1986–2017, Remote Sensing, 12, 10.3390/rs12162615, 2020.

Zhang, L., Gong, S., Padro, J., and Barrie, L.: A size-segregated particle dry deposition scheme for an atmospheric aerosol module, Atmospheric Environment, 35, 549-560, https://doi.org/10.1016/S1352-2310(00)00326-5, 2001.

Zhang, L., Jacob, D. J., Knipping, E. M., Kumar, N., Munger, J. W., Carouge, C. C., van Donkelaar, A., Wang, Y. X., and Chen, D.: Nitrogen deposition to the United States: distribution, sources, and processes, Atmos. Chem. Phys., 12, 4539-4554, 10.5194/acp-12-4539-2012, 2012.

Zhang, Q., Jia, S., Chen, W., Mao, J., Yang, L., Krishnan, P., Sarkar, S., Shao, M., and Wang, X.: Contribution of marine biological emissions to gaseous methylamines in the atmosphere: An emission inventory based on multi-source data sets, Sci Total Environ, 898, 165285, 10.1016/j.scitotenv.2023.165285, 2023.

Zhang, Z. and Yu, J. Z.: Quantifying sensitivity of PM2.5 mass to ammonia and nitrate availability in Hong Kong based on four-year hourly measurements, Environmental Science: Atmospheres, 6, 565-578, 10.1039/d5ea00114e, 2026.

Zhang, Z. E., Li, J., Zhang, R., Tian, C., Sun, Z., Li, T., Han, M., Yu, K., and Zhang, G.: Increase in Agricultural-Derived NH_x and Decrease in Coal Combustion-Derived NO_x Result in Atmospheric Particulate $N\text{-}NH_4^+$ Surpassing $N\text{-}NO_3^-$ in the South China Sea, Environ Sci Technol, 58, 6682-6692, 10.1021/acs.est.3c09173, 2024b.

Zhu, W., Shi, J., Guo, S., Wang, Q., Chen, J., Lou, S., and Hu, M.: Comparative analysis of methods for seasonal particulate organic nitrate estimation in urban areas, npj Climate and Atmospheric Science, 8, 21, 10.1038/s41612-025-00904-5, 2025.